Spectra of Heliumlike Krypton from Tokamak Fusion Test Reactor Plasmas

M. Bitter, H. Hsuan, C. Bush, S. Cohen, C. J. Cummings, B. Grek, K. W. Hill, J. Schivell, and M. Zarnstorff
Princeton University, Plasma Physics Laboratory, Princeton, New Jersey 08543

P. Beiersdorfer and A. Osterheld
University of California, Lawrence Livermore National Laboratory, Livermore, California 94550

A. Smith
Lock Haven University, Lock Haven, Pennsylvania 17745

B. Fraenkel
Hebrew University, Jerusalem, Israel
(Received 3 February 1993)

Experiments were conducted on TFTR to study the radiation of krypton which will be important for future tokamaks, such as ITER, for the diagnostic of the central ion temperature and for the control of the energy release from the plasma by radiative cooling. The total krypton radiation was monitored, and satellite spectra of Kr XXXV were recorded with a high-resolution crystal spectrometer. Radiative cooling and reduced particle recycling at the plasma edge region were observed, in reasonable agreement with modeling calculations which included radial transport.

PACS numbers: 52.20.Hv, 52.25.Jm, 52.70.La

Given the large plasma volume (500 m^3) and stored energy (600 MJ) specified for the International Thermonuclear Experimental Reactor (ITER) [1], the operation of ITER will face two major problems: (1) measurement of the central ion temperature $T_i(0)$ and (2) control of the energy release from the plasma under quasicontinuous conditions with pulse lengths ≥ 1000 s. To reduce the heat load on the plasma-facing components, it has recently been proposed to inject high-Z impurities into the plasma which can provide radiative cooling of the plasma edge region at a rate of 100 MW [2]. The most likely candidate is krypton, because it is chemically inert and easily injected in controllable amounts. Krypton can be used to solve both aforementioned problems: the radiation from the high charge state of heliumlike krypton, which will be the dominant state of ionization in the hot core of the plasma for the projected central electron temperatures of 10–30 keV, can be used for Doppler broadening measurements to determine $T_i(0)$, and the lower charge states of krypton can provide the required radiative cooling of the plasma edge and the divertor regions. In order to explore the potential of this experimental approach, it is necessary to study effects of the krypton injection on the plasma performance on present-day large tokamaks and to obtain accurate atomic physics data for *all* the krypton charge states [from theoretical calculations and experiments on atomic physics facilities like electron beam ion traps (EBIT)], since these data will be needed for plasma simulation calculations to predict the effects of radiative cooling. Another experimental challenge is the development of efficient crystal spectrometers at wavelengths of 0.95 Å, since the high spectral resolution ($\lambda/\Delta\lambda \geq 10000$) needed for Doppler broadening measurements may only be obtained in second-order Bragg reflection at the expense of a significant reduction in crystal reflectivity. In order to address these questions, which are crucial for the ITER performance as well as for the diagnostic of the central parameters of ITER plasmas, the International Atomic Energy Agency (IAEA) has recommended establishing an atomic physics database on krypton [3]. In this paper we present results from krypton experiments on TFTR. These experiments made it possible to study the performance of TFTR plasmas with krypton injection and to obtain high-resolution spectra of heliumlike krypton, Kr XXXV.

The experiments were conducted in Ohmically heated helium discharges with plasma currents, $I_p = 1.4$, 1.6, and 1.8 MA, electron densities in the range from 1.5×10^{19} to 2.5×10^{19} m^{-3}, and peak electron temperatures of 6 keV. The radial electron temperature profiles varied from a very peaked profile for $I_p = 1.4$ MA to a wide profile for $I_p = 1.8$ MA (see Fig. 1). Krypton was injected via a gas puff at the edge of these discharges at a rate of 0.2–0.35 Torr liter/s for time intervals of 0.2–0.25 s, after the plasma had reached steady state conditions. A survey spectrum of the emitted x-ray radiation from a discharge with $I_p = 1.8$ MA is shown in Fig. 2(a). The measurements were performed with the TFTR x-ray pulse height analysis (PHA) system [4]. The spectrum consists of a bremsstrahlung continuum and $K\alpha$-line radiation from various ions. The peak at 13 keV includes the $K\alpha$-line radiation from *all* the krypton charge states, since the energy resolution of the PHA system is only 230 eV. Figure 2(b) shows the observed time evolution of the brightness of the krypton $K\alpha$-line radiation for the investigated

0031-9007/93/71(7)/1007(4)$06.00

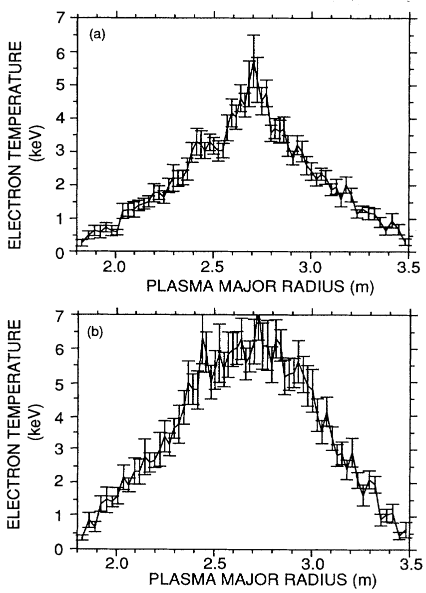

FIG. 1. Radial profiles of the electron temperature of Ohmically heated TFTR plasmas with different plasma currents: (a) $I_p = 1.4$ MA and (b) $I_p = 1.8$ MA, from laser Thomson scattering.

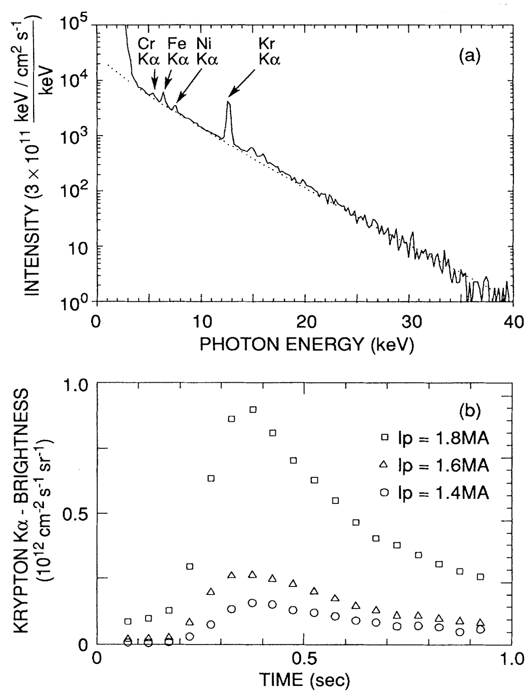

FIG. 2. (a) Survey spectrum of the x-ray radiation from a discharge with $I_p = 1.8$ MA. (b) Brightness of the krypton $K\alpha$ radiation as a function of time after the krypton injection.

discharges. From a further analysis of these PHA data, it is found that the total krypton density was ~0.1% of the electron density at the time of the maxima shown in Fig. 2(b). Measurements of the total radiated power were performed with the TFTR bolometer array [5] and are shown in Fig. 3. The additional total radiated power due to the krypton injection *decreased* from 1 to 0.6 MW for discharges with $I_p = 1.4$ MA and $I_p = 1.8$ MA, respectively, even though in the latter case a larger amount of krypton was injected, whereas the krypton $K\alpha$ radiation *increased* for increasing values of I_p [see Fig. 2(b)]. These results suggest that, for the broader electron temperature profiles obtained with $I_p = 1.8$ MA, the ionization equilibrium was shifted to the higher charge states, which emit significantly less line radiation than the lower states of ionization [6].

Predictions of the krypton ion charge state distribution and the radiated power profile were made using the MIST impurity transport code [7]. The modeling calculations were based on measured profiles of the electron temperature and density, the measured total krypton density of 0.1% of the electron density, and a constant diffusion coefficient of $D = 1$ m^2/s for all the krypton charge states. The following results were obtained: (1) The radial distribution of the krypton ion charge states was distinctly different for the three discharges, e.g., the central densities of Kr XXXV were 0.4×10^{15} m^{-3} for $I_p = 1.4$ MA and 2.0×10^{15} m^{-3} for $I_p = 1.8$ MA. (2) The calculated radial emissivity profiles of the total krypton line radiation were peaked for $I_p = 1.4$ MA, but hollow for $I_p = 1.8$ MA; and the central emissivities were distinctly different, e.g., 32 and 8 kW/m^3, respectively. (3) The calculated brightness of the heliumlike $K\alpha$ radiation was 3×10^{10} cm^{-2}s^{-1}sr^{-1} for $I_p = 1.8$ MA or 3% of the measured $K\alpha$ brightness shown in Fig. 2(b). (4) The total radiated power obtained from the volume-integrated krypton line

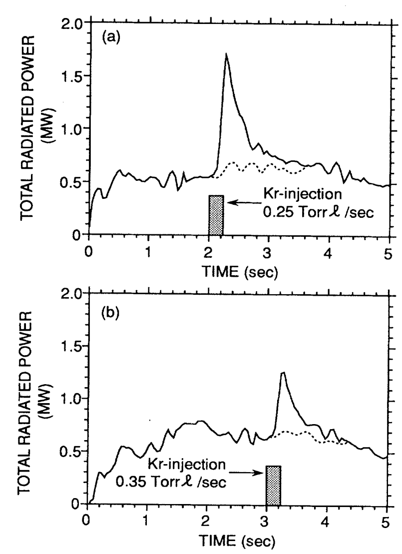

FIG. 3. Total radiated power for (a) $I_p = 1.4$ MA and (b) $I_p = 1.8$ MA. The dotted lines represent data from comparison discharges without krypton injection.

emissivities was $\Delta P_{rad}=0.96$, 0.81, and 0.46 MW for $I_p=1.4$, 1.6, and 1.8 MA, in reasonable agreement with the bolometer measurements. The result (2) may explain the measurements of the electron cyclotron emission (ECE), that showed a noticeable drop of the *central* electron temperature, $\Delta T_e(0)\sim -0.5$ keV, during the injection of krypton for $I_p=1.4$ MA, but $\Delta T_e(0)\sim 0$ for $I_p=1.8$ MA. Thus, in the latter case, the injected krypton did not perturb the core of the plasma. For all discharges, the ECE measurements showed a reduction of the *edge* electron temperature at $R=3.30$ m by 10% to 20% during the injection of krypton. This radiative cooling of the edge plasma was correlated with a reduction of the particle recycling between the wall and the edge plasma as indicated by a density decrease of 5% to 10% at $R=3.30$ m and a reduction of the edge-emitted carbon and $H\alpha$ light by more than 50%.

High-resolution spectra of krypton, which were used to test the feasibility of Doppler ion-temperature measurements, are shown in Fig. 4. The spectra were recorded with the TFTR vertical crystal spectrometer [8] using a 2023-quartz crystal (with $2d=2.7497$ Å and a curvature radius of 11.43 m) in second-order Bragg reflection at a Bragg angle $\Theta=43.7°$ to obtain a high spectral resolution of $\lambda/\Delta\lambda=12000$. The detector, a position-sensitive multiwire proportional counter (MWPC) with xenon as detector gas, was covered by aluminum foils [9] to attenuate the 6.5 keV photons, which were emitted from the bremsstrahlung continuum with a comparable or higher intensity than the 13 keV photons of interest [see Fig. 2(a)] and which were reflected in first order. The entire KrXXXV spectrum, which includes the heliumlike lines **w**, **x**, **y**, **z** and the associated lithiumlike, berylliumlike, and boronlike satellites, could only be observed from discharges with broad electron temperature profiles and is shown in Fig. 4(b). The spectral features have been identified using the instrumental dispersion and theoretical wavelengths from Ref. [10] and new HULLAC code calculations [11], and they are listed in Table I with the key letters according to Gabriel's notation [12]. We note that the lithiumlike and berylliumlike satellites are much closer to the resonance line **w** than in the previously studied spectra of heliumlike TiXXI, CrXXIII, FeXXV, and NiXXVII [8] as a result of Z-dependent wavelength shifts [13]. The forbidden line **z** is isolated and therefore well suited for Doppler broadening measurements, whereas the resonance line **w** seems to be blended with unresolved $n\geq 3$ satellites [14] and requires substantial corrections for ion temperature measurements. Indeed, least squares fits of single Voigt profiles to the lines **z** and **w** provided ion temperature values of 2.5 and 6.5 keV, respectively. The T_i value obtained from the line **z** is in reasonable agreement with the value of $T_i(0)=2.3$ keV, which was simultaneously measured from the FeXXV resonance line with a different channel of the TFTR vertical crystal spectrometer. The broadening due to $n\geq 3$ satellites should be significantly reduced for electron temperatures of $T_e\geq 10$ keV expected in ITER. The brightness of the heliumlike radiation on ITER will be 4 orders of magnitude larger than in the present experiments, according to MIST code modeling calculations which assumed an electron temperature of 20 keV, a density of 1×10^{20} m^{-3}, and a fractional krypton abundance of 0.1% [15]. Under these conditions, the count rate for the line **z** would increase from the current value of 60 to 3×10^5 s^{-1}, if the present spectrometer were used. This count rate is sufficient for time-resolved temperature measurements with a resolution < 50 ms. The fractional krypton abun-

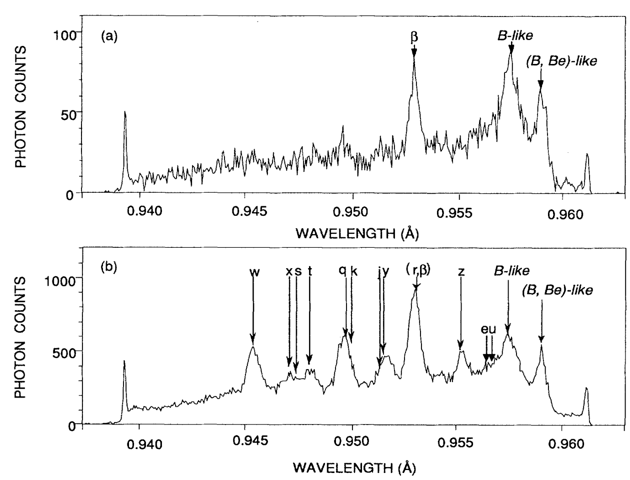

FIG. 4. Krypton $K\alpha$ spectra measured by the TFTR vertical crystal spectrometer with a vertical sightline through the center of the vacuum vessel at $R_0=2.65$ m. The data were accumulated (a) from 6 nearly identical Ohmic discharges with $I_p=1.4$ MA, and (b) from 18 nearly identical Ohmic discharges with $I_p=1.8$ MA.

TABLE I. Theoretical wavelengths for the transitions in heliumlike krypton, KrXXXV, and the main $n=2$ satellites.

Key	Transition	Wavelength (Å)
w	$\mathbf{1s^2\,{}^1S_0\text{-}1s2p\,{}^1P_1}$	0.945 38 [a]
x	$\mathbf{1s^2\,{}^1S_0\text{-}1s2p\,{}^3P_2}$	0.947 08 [a]
s	$1s^22s\,{}^2S_{1/2}\text{-}1s2p2s({}^3P)\,{}^2P_{3/2}$	0.947 46 [a]
t	$1s^22s\,{}^2S_{1/2}\text{-}1s2p2s({}^3P)\,{}^2P_{1/2}$	0.948 04 [a]
q	$1s^22s\,{}^2S_{1/2}\text{-}1s2p2s({}^1P)\,{}^2P_{3/2}$	0.949 61 [a]
k	$1s^22p\,{}^2P_{1/2}\text{-}1s2p^2\,{}^2D_{3/2}$	0.949 95 [a]
j	$1s^22p\,{}^2P_{3/2}\text{-}1s2p^2\,{}^2D_{5/2}$	0.951 37 [a]
y	$\mathbf{1s^2\,{}^1S_0\text{-}1s2p\,{}^3P_1}$	0.951 56 [a]
r	$1s^22s\,{}^2S_{1/2}\text{-}1s2p2s({}^1P)\,{}^2P_{1/2}$	0.952 88 [a]
β	$1s^22S^2\,{}^1S_0\text{-}1s2p2s^2\,{}^1P_1$	0.9529 [b]
z	$\mathbf{1s^2\,{}^1S_0\text{-}1s2s\,{}^3S_1}$	0.955 25 [a]
e	$1s^22p\,{}^2P_{3/2}\text{-}1s2p^2\,{}^4P_{5/2}$	0.956 15 [a]
u	$1s^22s\,{}^2S_{1/2}\text{-}1s2s2p({}^3P)\,{}^4P_{3/2}$	0.956 52 [a]

[a]Reference [10].
[b]From present calculations.

dance in ITER could therefore be reduced to less than 0.1% of the electron density. We also note that the throughput of crystal spectrometers could be further improved by using doubly focusing crystals and more efficient detectors for the 13 keV photons.

In conclusion, experiments were performed on TFTR to explore the effects of krypton on the plasma performance and to study the emitted line radiation of krypton, which is of interest for future tokamaks, such as ITER, both for the diagnostic of the central ion temperature and for the control of the energy release from the plasma. Bolometer measurements of the total radiated power and measurements of the krypton $K\alpha$-line radiation indicate that the spectrum of the emitted krypton radiation depends very sensitively on plasma parameters, such as the electron temperature profile. A high-resolution crystal spectrometer was used to measure the line radiation of the heliumlike, lithiumlike, and berylliumlike krypton charge states in second-order Bragg reflection. Although heliumlike krypton was only marginally present in all investigated cases, it was possible to record the entire satellite spectrum of Kr XXXV. The forbidden line **z** appears to be free from satellites and therefore well suited for ion-temperature measurements. The injection of krypton also produced a decrease of the plasma edge electron temperature and density, indicating effects of radiative cooling and reduced particle recycling. Modeling calculations of the krypton ion charge state distribution including transport effects and calculations of the total power of the emitted krypton line radiation are in reasonable agreement with the observations. Comparison of the present results with quantitative estimates of the signal strengths from ITER indicate that the count rate for the line **z** will be sufficient for time resolved ion-temperature measurements with a resolution of 50 ms at krypton densities less than 0.1% of the electron density. These amounts of krypton will provide edge cooling at a rate of ~100 MW without perturbing the core of ITER plasmas. In order to determine the effects of krypton radiation for different experimental conditions on ITER and to develop the injection of krypton as a tool for the control of the energy release and diagnostic of central plasma parameters on ITER, theoretical atomic physics studies, experiments on atomic physics facilities, and further tokamak experiments are needed. These first experimental results from TFTR should stimulate further research in these areas.

We are grateful to Dr. A. Henins from the National Institute of Standards and Technology, Gaithersburg, Maryland, for providing us with information on crystal properties. We also gratefully acknowledge the continuing support of R. J. Hawryluk and K. M. Young as well as the technical assistance of J. Gorman, R. Such, and the TFTR operating crew. This work was supported by the U.S. Department of Energy, Contract No. DE-AC02-76-CHO-3073.

[1] K. Tomabechi *et al.*, Nucl. Fusion **31**, 1135 (1991); *ITER Operations and Research Programme*, ITER Documentation Series No. 23 (International Atomic Energy Agency, Vienna, 1991).

[2] C. J. Cummings, S. A. Cohen, R. Hulse, D. E. Post, and M. Redi, J. Nucl. Mater. **176 & 177**, 916 (1990).

[3] IAEA Technical Committee Meeting on Atomic and Molecular Data for Fusion Reactor Technology Cadarache, France, 12–16 October 1992.

[4] K. W. Hill, M. Bitter, M. Diesso, L. Dudek, S. von Goeler, S. Hayes, L. C. Johnson, J. Kiraly, E. Moshey, G. Renda, S. Sesnic, N. R. Sauthoff, F. Tenney, and K. M. Young, Rev. Sci. Instrum. **56**, 840 (1985).

[5] J. Schivell, G. Renda, J. Lowrence, and H. Hsuan, Rev. Sci. Instrum. **53**, 1527 (1982); J. Schivell, *ibid.* **56**, 972 (1985).

[6] D. E. Post, R. V. Jensen, C. B. Tarter, W. H. Grasberger, and W. A. Lokke, At. Data Nucl. Data Tables **20**, 397 (1977).

[7] R. A. Hulse, Nucl. Technol. Fusion **3**, 259 (1983).

[8] M. Bitter, H. Hsuan, J. E. Rice, K. W. Hill, M. Diesso, B. Grek, R. Hulse, D. W. Johnson, L. C. Johnson, and S. von Goeler, Rev. Sci. Instrum. **59**, 2131 (1988).

[9] The aluminum foils (total thickness 0.008 in.) were chosen to compensate for the effects that the integrated crystal reflectivities for first- and second-order Bragg reflection differed by 1 order of magnitude ($R_c = 4.17 \times 10^{-6}$ rad for the 6.5 keV photons and $R_c = 0.44 \times 10^{-6}$ rad for the 13 keV photons) and that the detector efficiency for these photons differed by a factor of 2.5 (100% and 40% for photons of 6.5 and 13 keV, respectively).

[10] L. A. Vainshtein and U. I. Safronova, P. N. Lebedev Institute of Spectroscopy Report No. 2, 1985.

[11] M. Klapisch, Comput. Phys. Commun. **2**, 239 (1971); M. Klapisch, J. L. Schwob, B. S. Fraenkel, and J. Oreg, J. Opt. Soc. Am. **61**, 148 (1977).

[12] A. Gabriel, Mon. Not. R. Astron. Soc. **160**, 99 (1972).

[13] TFR group, M. Cornille, J. Dubau, and M. Loulergue, Phys. Rev. A **32**, 3000 (1985).

[14] P. Beiersdorfer, S. Chantrenne, M. H. Chen, R. E. Marrs, D. A. Vogel, K. L. Wong, and R. Zasadzinski, Z. Phys. D **21**, 209 (1991).

[15] K. W. Hill, K. M. Young, M. Bitter, S. von Goeler, H. Hsuan, R. Hulse, L.-P. Ku, B. Stratton, A. S. Krieger, D. Parsignault, and E. D. Franco, Rev. Sci. Instrum. **63**, 5032 (1992).